Available online at www.sciencedirect.com
SCIENCE DIRECT
Sensors and Actuators B 107 (2005) 882–891
SENSORS AND ACTUATORS B CHEMICAL
www.elsevier.com/locate/snb

Microfabrication and characterization of a silicon-based millimeter scale, PEM fuel cell operating with hydrogen, methanol, or formic acid

J. Yeom[a], G.Z. Mozsgai[a], B.R. Flachsbart[a], E.R. Choban[b], A. Asthana[b], M.A. Shannon[a,1], P.J.A. Kenis[b,*]

[a] Department of Mechanical & Industrial Engineering, University of Illinois, Urbana, IL 61801, USA
[b] Department of Chemical & Biomolecular Engineering, University of Illinois, Urbana, IL 61801, USA

Received 16 July 2004; received in revised form 25 November 2004; accepted 9 December 2004
Available online 29 January 2005

Abstract

A silicon-based microfabricated fuel cell has been developed to provide a high energy and power density power source on the millimeter size scale. An integrated silicon microscale membrane electrode assembly (Si-μMEA) consisting of a Nafion 112™ membrane bonded between two electrodes on microstructured silicon substrates forms the core element of this polymer electrolyte membrane fuel cell. The use of silicon meshes that serve the purpose of catalyst support, current collector, and structural element provides a promising alternative to the traditional gas diffusion layer-based MEAs for the development of robust, high-performance microfuel cells. The cell performance was characterized using hydrogen, methanol, and concentrated formic acid–water fuels at the anode, and oxygen at the cathode. The catalyst used for each fuel was Pt black. Preliminary results show that the microfabricated fuel cell running on formic acid may be a promising alternative for fuel cell applications running at ambient temperature and pressure, provided additional work on catalyst improvement, assembly, and packaging is performed so that the power density achieves that of traditional forced fed PEM fuel cell design.

Keywords: Microfuel cell; Membrane electrode assembly; Formic acid; Portable power sources; Microfabrication

1. Introduction

Recently, microfabricated polymer electrolyte membrane (PEM) fuel cells are being developed by many research groups to generate power for MEMS and IC devices [1–17]. The proliferation of portable electronic devices such as cellular telephones, PDAs, laptops, etc. has led to an increased demand for cheap, efficient, and lightweight power sources. Moreover, very small systems that employ MEMS sensors, actuators, and RF communications are being developed for large-scale distributed networks. A major problem for these MEMS devices is that they need to operate for sustained periods of time (longer than 30 days) with relatively high power demands on the order of milliwatts. These criteria are driving the development of both high energy (1 KJ/cm^3) and power density (10 W/cm^3) on-chip electrical sources [6]. This paper reports on the design, fabrication, and characterization of a silicon-based microfabricated fuel cell as a high energy and power density power source on the millimeter size scale.

Unfortunately, batteries, while ideal for supplying solid-state electrical power, are often limited in the ability to simultaneously deliver high energy and power densities, and a great deal of research and development has been expended to continuously improve their performance [18]. Microfabricated fuel cells may offer another solution, if some of the substantial challenges faced in supplying both high energy and power densities are solved. To supply both high energy and power density, fuel cell systems are often operated at elevated temperatures and pressures [19]. Also, these fuel cell systems

* Corresponding author. Tel.: +1 217 265 0523; fax: +1 217 333 5052.
E-mail addresses: mshannon@uiuc.edu (M.A. Shannon), kenis@uiuc.edu (P.J.A. Kenis).
[1] Tel.: +1 217 244 1545.

0925-4005/$ – see front matter
doi:10.1016/j.snb.2004.12.050

often utilize ancillary equipment such as heaters, pumps, fuel reformers, and water and air management systems to address specific issues and problems encountered with fuel cells. Such ancillary devices can be difficult to scale down in size with a proportionate decrease in energy consumption due to parasitic loses. The total percentage of parasitic losses often increases as size decreases, reducing energy and power densities attainable. Minimizing ancillary systems, therefore, is one of our goals in developing an on-chip fuel cell.

The fuel used in fuel cell systems sets the upper limits of power and energy densities that can be achieved. For instance, hydrogen gas is known to be a high power but low energy density fuel unless packaged under very high pressures. The use of liquid fuels such as methanol (MeOH) can potentially achieve several orders of magnitude higher energy density than H_2. However, slow oxidation reaction kinetics at ambient conditions and severe fuel crossover through the Nafion membrane that typically separates the anode and cathode, reduce the actual performance from the theoretical. Kelley et al. demonstrated miniaturized direct methanol fuel cells (DMFC) in 2000 [1,2] with a performance comparable to traditional large-scale systems. Other miniature fuel cells and design approaches have also been studied [3–8], where most of these approaches have used methanol as a fuel and were not necessarily post-CMOS compatible. Shah et al. fabricated a Si- and Nafion membrane-based FC using micromachining technology [9]. More recently, Shah et al. also utilized PDMS and soft lithographic techniques to develop a polymer-based microPEM fuel cell [10].

Rice et al. [20] and Ha et al. [21] have demonstrated the potential of HCOOH as a fuel in a traditionally manufactured PEM fuel cell, in particular its advantages over methanol when operated at room temperatures. Although it has lower energy density than MeOH (50% less comparing neat solutions), formic acid's higher reaction kinetics can yield over three orders of magnitude gains in power density. Additionally, reduced fuel crossover allows formic acid fuel cells to be run at much higher concentrations (20–80%) versus MeOH (∼6%), which can potentially lead to higher fuel mixture energy densities, and thus fuel cell systems with a higher power density (or a smaller fuel cell system to provide the same power). Zhu et al. reported that in a traditionally manufactured flow-through fuel cell, 3 M formic acid provided 84 mA/cm^2 at 0.3 V and 18 °C with a forced oxygen stream at the cathode [22], while the same cell run with 1 M MeOH as the fuel under the same conditions only provided 45 mW/cm^2 at 0.2 V. This gain is a key to the usefulness of such a miniaturized cell. Most importantly, retaining the ability to supply high power densities at ambient temperature and humidity as well as to eliminate many ancillary systems is crucial for an on-chip microfuel cell. Choban et al. have also used formic acid as a fuel in membraneless fuel cells that exploit laminar flow to keep the cathodic and anodic streams separate yet in diffusional contact [8].

A particularly troubling problem with DMFCs is the crossover of methanol through the Nafion membrane from the anode to the cathode, causing a mixed potential and the subsequent drop in cell performance. In contrast, HCOOH crossover through Nafion membranes as a result of natural diffusion seems to be considerably lower at room temperature, yet these measurements do not account for electroosmotic drag [25]. Crossover of formic acid through a membrane electrode assembly (MEA) in a working fuel cell system has not yet been quantified, and cannot be ruled out based on our data. Low open-circuit cell potential is one indicator of such a mixed potential, which will be discussed later.

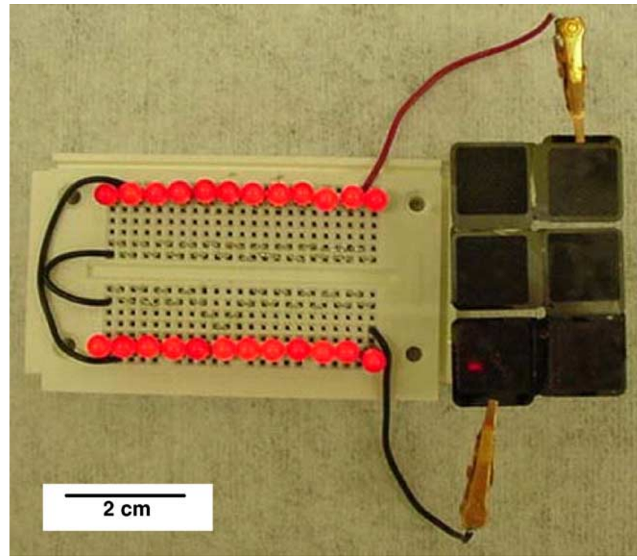

Fig. 1. A photograph of six Si-μMEAs in operation with 10 M HCOOH as the liquid fuel passively delivered to anode and oxygen from the air as the oxidant illuminating LEDs at room temperature.

This paper reports the design, fabrication, and performance of a monolithic silicon-based microscale membrane electrode assembly (Si-μMEA) consisting of an integrated metallic current collector and a standard Nafion membrane with microfabricated Si structural elements. This integrated Si-μMEA represents a promising alternative to traditional multilayer gas diffusion MEAs in the development of robust, high-performance microfuel cells. Miniature fuel cells were successfully fabricated using silicon microfabrication techniques adapted from the MEMS and microelectronic industries (Fig. 1). Room temperature fuel cell performance characteristics for three fuel–oxidant combinations will be presented and the performance limitations of these Si-μMEAs as well as further opportunities to increase their performance will be discussed.

2. Experimental

The Si-μMEA is comprised of two silicon electrodes, with catalyst deposited directly on them, supporting a Nafion 112^{TM} membrane between them. The two electrodes are identical gold-covered Si structures, where the Au layers serve as the current collector and are covered with

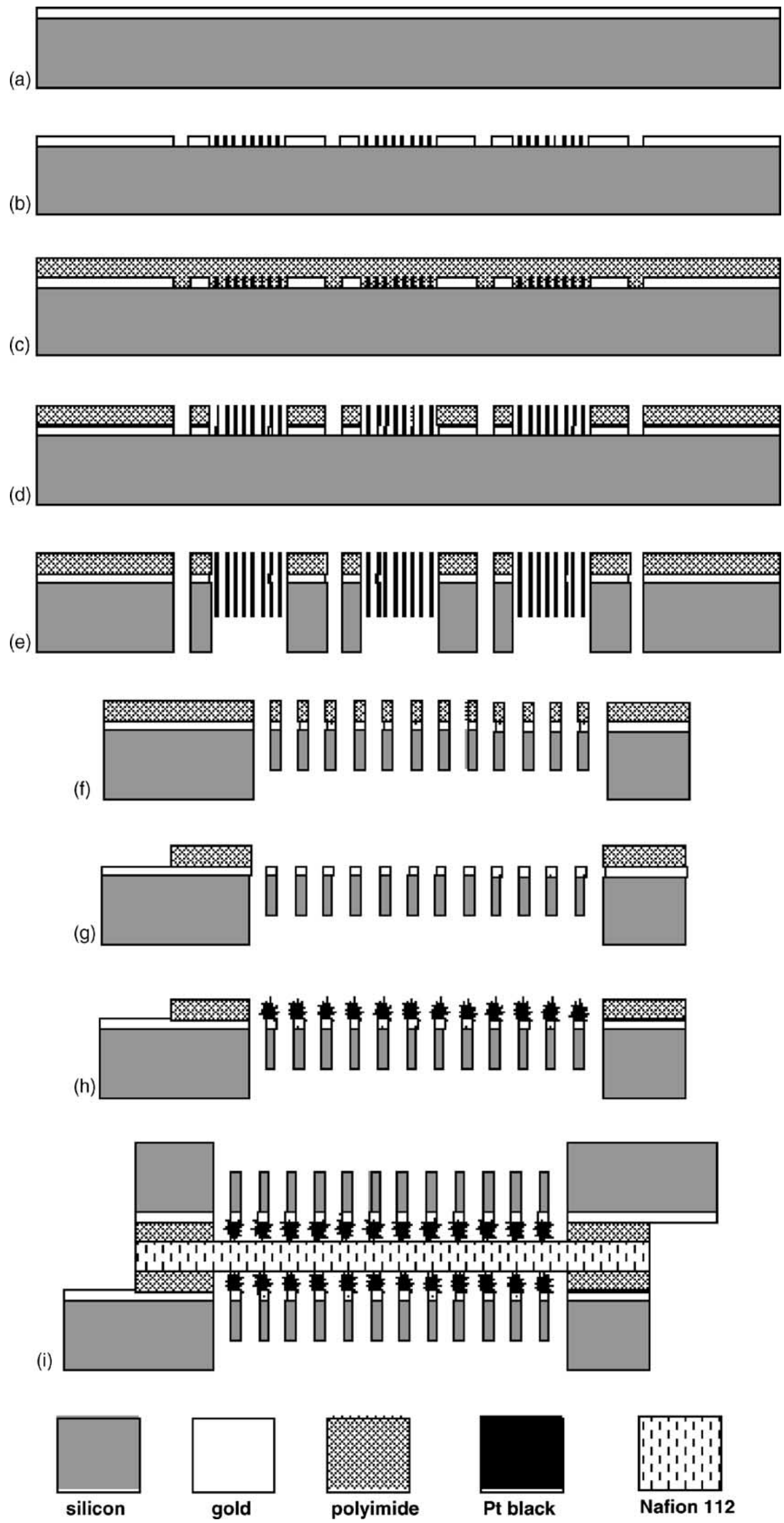

Fig. 2. Schematic of the Si-μMEA fabrication process: (a) sputter Au layer on double-side polished wafer; (b) pattern Au layer with liftoff process; (c) spincoat and cure a polyimide layer; (d) perform the double-sided photolithography to pattern etch pits; (e) etch Si in ICP-DRIE to form Au/Si electrode; (f) dice the wafer into a single die; (g) RIE etch the polyimide layer with a shadow mask to expose current collecting region; (h) electroplate Pt black on Au layer; (i) sandwich both electrodes with Nafion 112 in a hot press bonder.

electrodeposited Pt black catalyst for both the anode and cathode. A schematic of the processing sequence for the fabrication and assembly of the Si-μMEA is shown in Fig. 2.

2.1. Fabrication of silicon electrode grids

The Si-based electrode structures were fabricated using traditional MEMS fabrication processes from a 100 mm double-side polished wafer (Silicon Quest, 500 μm thick, ⟨1 0 0⟩ oriented, 100 Ω cm of the nominal resistivity). To enhance the current collection of the silicon electrodes, a 1000 Å Au layer with a 100 Å Cr adhesion layer was deposited using DC magnetron sputtering (∼10^{-2} Torr of Ar background pressure) and patterned with a liftoff process.

The front of the wafer was coated with a PMDA-ODA polyimide layer (PI-2808, HD Microsystem) used as an adhesion and spacer layer between the silicon die and the nafion membrane. The spacer layer is required to accommodate the volume of the catalyst that is grown up from the surface of the current collector. In addition, the polyimide film in combination with a native oxide serves to electrically isolate the cell halves. The film is deposited by spincoating polyamic acid and then thermally imidized under vacuum. The polyimide layer was patterned using photolithography and subsequent RIE to form the mask for etching the silicon. In the second photolithographic process, the front pattern was aligned to the etch pits on the back of the wafer. The grid-like Si structure of the electrodes was etched through using ICP-DRIE (Plasma-Therm SLR 770) to form a mesh with 50 μm wide ribs separated by a 150 μm pitch. The polyimide layer is then removed from the electrode region as well as the contact pads to expose the Au layer. The polyimide etching is accomplished with an oxygen plasma in the RIE system (March Instruments, Jupiter III) using a silicon shadow mask.

A catalytic layer of Pt black was electroplated directly onto the current collector to create a direct electron-conducting path between the catalyst and the current collector. The direct path is intended to reduce the contact and bulk resistance losses within the cell versus traditional catalyst inks applied to the membrane. The plating bath consisted of 120 ml of DI water, 5 g of dihydrogen hexachloroplatinate ($H_2PtCl_6 \cdot 6H_2O$, Alfa AESAR), and 30 mg of lead acetate ($(Pb(CH_2COOH)_2 \cdot 3H_2O$, Alfa AESAR). The amount of Pb incorporated into the final dendritic Pt structures was below the detection limit of XPS, and thus negligible. High surface area structures were achieved by carrying out the deposition at relatively high current densities of about 1 A/cm^2.

2.2. Silicon-μMEA preparation

The two Si electrodes and Nafion membrane are sandwiched and hot-pressed to form the membrane electrode assembly, where a PI adhesion promoter (VM652, HD Microsystem) was employed at the interface promoting the adhesion between the Nafion membrane and the PMDA-ODA surface. The membrane electrode assembly was bonded at 120 °C under a pressure of ∼200 N/cm^2 in the EV-420 bonder. Prior to bonding, the Nafion 112^{TM} membrane (Fisher Scientific) was protonated by soaking it at 80 °C in sequence in dilute H_2O_2, DI water, dilute H_2SO_4, and DI water for 1 h each. Following assembly, the complete Si-μMEAs were stored in DI water to keep the membranes hydrated.

2.3. Fuel cell testing setup

The cell was tested with a custom-built fuel cell testing system as shown in Fig. 3. Gases (H_2 and O_2) are delivered to the cell through mass flow controllers (MKS, MC20) and humidifiers (bubbling through water). The cell is mounted in a glass-filled Teflon^{TM} composite test fixture (PTFE, K-mac Plastics) that facilitates gas flow over the electrode surfaces as well as electrical interconnection of the current collector through jumper contacts. Voltage and current measurements were performed utilizing LabView 5.0 software coupled to a National Instruments Field Point DAQ system, which is also used to regulate the load on the cell. Current–voltage

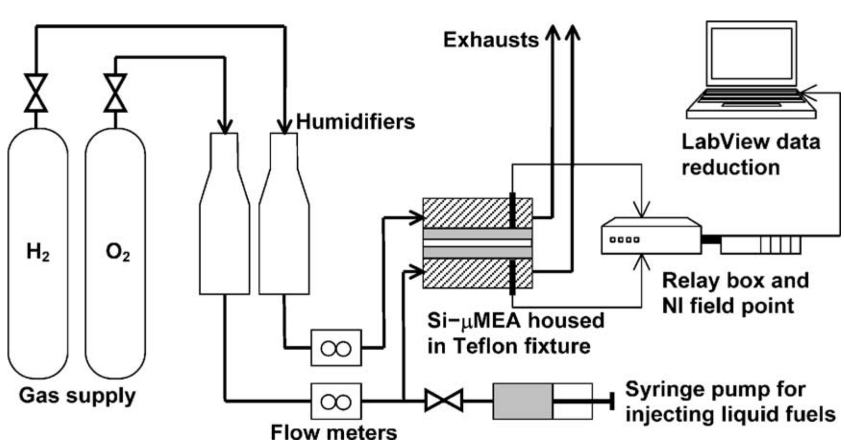

Fig. 3. A schematic of the Si-μFC test apparatus. It can supply dry or humidified oxygen, air, hydrogen, liquid methanol, formic acid and water to the Si-μFC cells. Current control is achieved by supplying opposing voltage bias to the cell, which is recorded by computer.

curves were generated by recording data points for a number of different loads from the open cell to 0 V, while allowing the system to reach steady state before recording data points. All tests were performed near room temperature (~20 °C) following a preconditioning routine that consisted of operating the cell with H_2 and O_2 at no load conditions for 15 min, followed by 15 min at short circuit. This sequence was repeated twice. The preconditioning was required to hydrate the membrane, as significant drying occurs during the bonding process.

Following preconditioning, the cell was tested using three different combinations of fuel and oxygen. The formic acid (ACS grade, 96% from ACROS) solutions and the methanol (Fischer) solutions were obtained by dilution with DI water. The liquid fuels were delivered to the anode with a syringe pump (PHD 2000 i/w, Harvard Apparatus) through the glass-filled Teflon™ composite test fixture. Both H_2 and O_2 gas were regulated with flow controllers (MKS, MC20) and passed through a 18.3 MΩ cm Millipore water to humidify the streams before delivery to the Si-μMEA. When testing the Si-μMEA with the liquid fuels (MeOH and HCOOH), higher oxygen flow rates were used to ensure that the cell would not be limited by oxygen transport on the cathode side. All errors in each point reported in the *IV* plots are estimated as ±5%.

3. Results and discussion

3.1. Design of fuel cell electrodes

Though microfabrication techniques have been used to create the miniaturized structures for the fuel cell components, the deposition of the catalyst layer is usually done on the electrolyte membrane by means of painting, screen-printing, and spraying inks containing a mixture of electrolyte and carbon-supported catalysts [12–14,26]. These methods are adapted from the traditionally manufactured gas diffusion layer-based MEAs for large-scale PEM fuel cells and are not typical of microfabrication processes employed in wafer scale MEMS fabrication. In this work, we fabricated an entire wafer of MEA dies with integrated catalyst in batch mode by electroplating the catalyst directly onto the current collector, without handwork or single process catalyst application. Table 1 compares some of the main design, operation, and performance differences between traditional PEMFC designs and the Si-μMEA-based fuel cell design studied in this work. Fig. 4(a) shows a photograph of a fully integrated Si-μMEA. A scanning electron microscope (SEM) image of a silicon electrode substrate grid is shown in Fig. 4(b). An array of 100 μm square holes in the electrode structures may facilitate (i) reduction in the transport resistance of fuel to the catalyst and (ii) rapid transport of CO_2 generated at the anode from the interface. Another advantage of our Si-μMEA structures is the ease in fabricating and assembling due to the fact that the current collector, catalyst support, and fuel/oxidant delivery structure are all integrated in one chip. Similar electrode designs for the microscale fuel cells were reported previously using anisotropic wet etching of Si [1,11]. The thickness of the electrode substrate mesh can be characterized by controlling the DRIE etching time. The thinner the Si supporting structure can be made, the faster the fuel and products can be transported to and from the electrode, but the poorer structural integrity will be. A 50 μm wide and 50 μm thick electrode substrate mesh was chosen for our Si-μMEA as a compromise for handling strength and utility versus thinness.

Another issue in optimizing the Si-μMEA performance is related to the thickness of the polyimide spacer layer. The distance between the catalyst layer and the Nafion membrane can be adjusted by the thickness of polyimide layer, determining how well the catalysts structures are in contact and/or penetrating the Nafion membrane. Si-μMEA with two different thicknesses (2 and 5 μm) of polyimide layers are tested and compared using the H_2 and O_2 as the fuel and oxidant, respectively (vide infra). Fig. 4(c) illustrates the SEM images of Pt black catalyst directly deposited by electroplating on the metal-covered Si grid shown in Fig. 4(b). The exploded view in Fig. 4(d) suggests a high-density Pt deposition (dendritic Pt). The electrodeposited Pt catalyst

Table 1
Summary of properties and characteristics of individual cells of microscale fuel cells based on PEM FC and Si FC technology using methanol (M) or formic acid (FA) as the fuel

Fuel cell type		PEM-based FC (DMFC or DFAFC)	Si-μMEA-based FC (Si DMFC or Si DFAFC)
Design	MEA components	Serpentine channels (1), current collector (2), carbon cloth (3), Nafion membrane	Single Si die, Nafion membrane
	Assembled MEA	Stack of MEA components by clamping	Sandwich of 2 Si dies and Nafion membrane by hot pressing
Operation	Primary fuels	MeOH or HCOOH	MeOH or HCOOH
	Fuel delivery	Forced liquid feed [22]	Quiescent or forced (this work) liquid feed, vapor feed
	Catalyst	Pt, Pt/Ru, Pt/Pd	Pt (this work), Pt/Pd
	Fuel concentration	MeOH (~3 M), HCOOH (5–12 M)	MeOH (1–3 M), HCOOH (5–12 M)
	Operating temperature	25–60 °C	25 °C (room temperature)
	Oxidant	Forced O_2, quiescent air	Forced O_2, quiescent air
	Product water management	Possible evaporation of excess H_2O at cathode	Possible evaporation of excess H_2O at cathode
Performance	Power density (mW/cm^2)	~100 at 0.3 V, MeOH [24]	~20 at 0.2 V, FA (non-optimized)

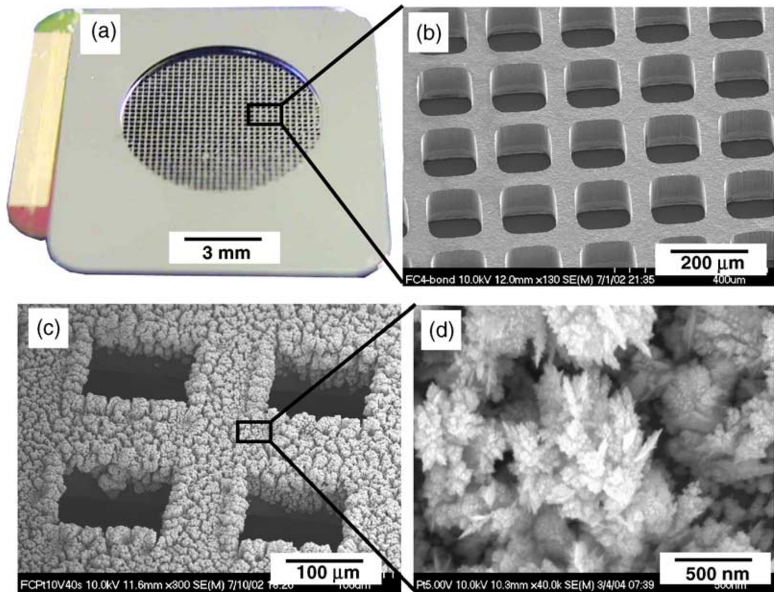

Fig. 4. Images of the Si-μMEA: (a) a photograph of a completely bonded MEA; (b) SEM micrograph of the silicon electrode structure etched in DRIE; a 50 μm thick electrode mesh with an array of 150 μm wide square holes; (c) SEM micrograph of the Pt catalyst deposited directly onto the Au-covered silicon mesh; (d) SEM micrograph of the electrodeposited Pt black structure with a roughness factor of about 500.

layer exhibits two distinct structures: open pore structures on the microscale and dendritic surface structure on the nanoscale. The dendritic growth of Pt black catalyst is not uniform and its thickness varies from 3 to 5 μm. The surface area of these structures was determined from the area under the H_2 adsorption/desorption curve obtained with cyclic voltammetry and then dividing this area by the catalyst loading. A surface area of 9.7–12.3 m^2/g was typically obtained, which corresponds to a roughness factor of about 500.

Different ways to apply the catalyst material to form MEAs in microscale fuel cells include evaporation, sputtering, and electroplating, common techniques in the microelectronic industry. The catalyst layer, commonly Pt, is sputtered or evaporated on the polymer electrolyte membrane serving as a current collector simultaneously [15,16]. Shah et al. deposited electrodes and catalysts on both sides of the Nafion membrane by sputtering using elastomeric shadow mask of PDMS to achieve better utilization of the catalyst with very low catalyst loading [10]. They employed a micro-patterned electrode structure on the membrane surface of a thin layer of catalyst (Pt or Pd) together with a thick patterned structure of other conductive material as a current collector to minimize series and contact resistance and to allow sufficient open surface for reactant gas to access and diffuse through the active catalyst sites. Sputtered catalyst, however has a very low surface area and thus yields fewer catalytically active sites.

An electroplated catalyst layer on the metal current collector in our Si-μMEA exhibits some advantages over other methods reviewed. The catalyst was grown on the current collector and then was subsequently bonding to the membrane leaving all three parts intimately connected. Therefore, upon dissociation of the hydrogen ion on the catalyst surface, the proton would have no more than a few microns to travel before reaching the membrane. Similarly, upon ionization, the freed electron is conducted directly through the catalyst and into the current collector, without having to conduct through Nafion ink or other contact barriers. This direct conduction path reduces the resistive loss associated with traditional fuel cell designs.

Fabricating the current collector out of gold rather than carbon cloth further reduces transport resistance. Carbon cloth was first used in H_2 fuel cells to carry current while allowing the gaseous fuel, oxygen, and byproducts to diffuse through the current collectors en route to the catalytic surfaces at the anode and cathode. Due to the low viscosity of H_2 and O_2, the resistance of transport through the carbon cloth is very low. However, in viscous liquids, carbon cloth can add extra resistance to transport of active species at the anode. In our Si-μMEA, the carbon cloth is replaced with Au and dendritic Pt, resulting in easy wetting of the metal surfaces by liquids such as water, formic acid, and methanol. Consequently, these fuels will easily wick through the catalyst-covered Si grid/current collector to the PEM. The effective surface area of the single Si-μMEA was measured to be 0.44 cm^2. A drawback of this approach is that the Pt loading of SiFC is higher than desired, approximately 2.5 mg/cm^2. A new process for Pt deposition is currently under development to lower Pt loading to less than 0.5 mg/cm^2. Current–voltage characteristics of cells comprised of identical Si-μMEAs with the three different fuel–oxidant combinations of hydrogen–oxygen, methanol–oxygen, and formic acid–oxygen can be performed as discussed next. Differences and similarities in operation between traditional PEMFCs and the Si-μMEAs studied here are listed in Table 1.

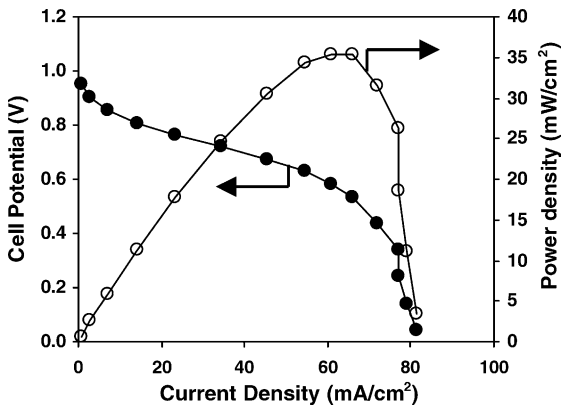

Fig. 5. *IV* (dark circle) and power density (clear circle) profiles of a Si-μFC operating with 7 ml/min of humidified hydrogen and 7 ml/min of humidified oxygen at room temperature and atmospheric pressure. The distance between the Au electrode and the Nafion membrane is 2 μm. The error in each point is estimated as ±5%.

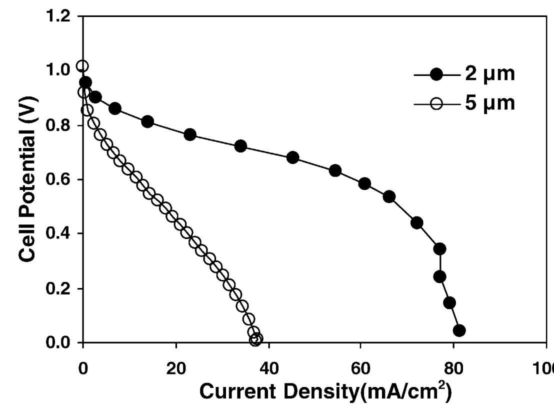

Fig. 6. *IV* curves of Si-μFCs for a different thickness of the polyimide spacer layer between the Au electrode and the Nafion membrane under the same operating condition: 7 ml/min of humidified hydrogen and 7 ml/min of humidified oxygen at room temperature.

3.2. Performance: hydrogen–oxygen testing

The hydrogen–oxygen reactive couple has the simplest and best understood reaction mechanism. Therefore, hydrogen–oxygen tests were carried out to provide a baseline of cells performance. Fuel cell performance was tested with hydrogen and oxygen flow rates of 7 ml/min. Both fuel and oxidant streams are humidified by leading the streams through Millipore water as explained in Section 2.

An open cell potential (OCP) of 1 V was measured while operated at room temperature (Fig. 5). With the theoretical electromotive force (EMF) of the reaction pair being 1.23 V, the cathode overpotential can be responsible for at most a 0.23 V drop in cell potential. Considering that the cell is operated at room temperature, the cell performance is comparable to other miniaturized PEM fuel cells reported earlier [2,12]. From Fig. 5, the abrupt potential drop in the high current regime suggests an oxygen transport limitation on the cathode side, since on the anode side Pt black is an excellent catalyst for H_2 in anode. The electrodeposited catalyst exhibits excellent wettability, which, however, generates an excess of water on the cathode thereby blocking oxygen transport to the catalyst. At room temperature, a maximum power density of 35 mW/cm^2 was achieved (Fig. 5) at 0.6 V.

As shown in Fig. 6, different performances have been observed for the different thicknesses of the polyimide spacer layer under the same testing condition (hydrogen and oxygen flow rates each 7 ml/min at room temperature). A large increase in performance of a thinner spacer layer (2 μm) is attributed to the fact that the shorter distance between the Au electrode and the Nafion membrane ensures a more intimate contact of the catalysts grown on the Au electrode into the electrolyte membrane. Therefore, balancing should take place between the height of the catalysts grown and the thickness of the polyimide layer. Due to the superior performance seen in the H_2–O_2 testing, the subsequent testing on the two liquid fuels, MeOH and HCOOH, was performed with a Si-μMEA with a 2 μm polyimide layer.

3.3. Performance: MeOH–oxygen testing

The methanol oxidation reaction at the anode has been studied extensively, since the DMFC gained significant attention as a special form of a low temperature PEM fuel cell [19]. The overall reaction at the anode is

$$CH_3OH + H_2O \rightarrow CO_2 + 6H^+ + 6e^- \quad (1)$$

with a number of different reaction pathways occurring to varied degrees depending on the potential [27]. Note that this reaction requires water to oxidize carbon to CO_2, and that CO is formed as an intermediate in the electro-oxidation of the methanol atom. CO is a known catalyst poison, which reduces the catalytic activity [20,27].

A Si-μMEA, identical to those used for H_2–O_2 tests, with a 2 μm polyimide layer, was operated with 1.25 M methanol solution at a flow rate of 1 ml/min as the fuel and humidified oxygen at a flow rate of 90 ml/min as the oxidant. Similar performance characterizations were carried out with a 10 M formic acid solution as the fuel. In these tests, the oxygen flow rate was increased from 7 to 90 ml/min to assure that there were no mass transport limitations at the cathode, and so, the cell performance would be anode limited. A maximum OCP of 0.42 V was observed, while the EMF of the methanol–oxygen reaction pair is 1.18 V. This low OCP and an abrupt initial drop of voltage in the low current density regime suggest that the fuel cell is anode limited. A maximum power density of 0.38 mW/cm^2 was obtained at 0.15 V (see Fig. 7). Although the current densities are significantly lower than in the H_2–O_2 case, the cell's room temperature performance with MeOH is much higher than the performance of other microscale DMFCs previously reported [4,5,16]. The low performance is attributed primarily to the slow room temperature decomposition kinetics of MeOH as well as CO poisoning of the Pt catalysts [4,20].

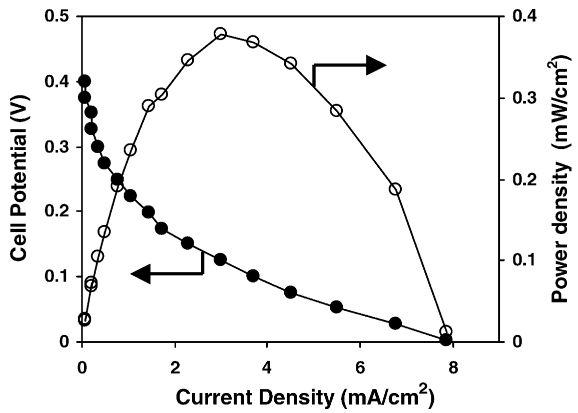

Fig. 7. *IV* (dark circle) and power density (clear circle) profiles of a Si-μFC operating with 1 ml/min of 1.25 M MeOH and 90 ml/min of humidified oxygen at room temperature and atmospheric pressure. The distance between the Au electrode and the Nafion membrane is 2 μm.

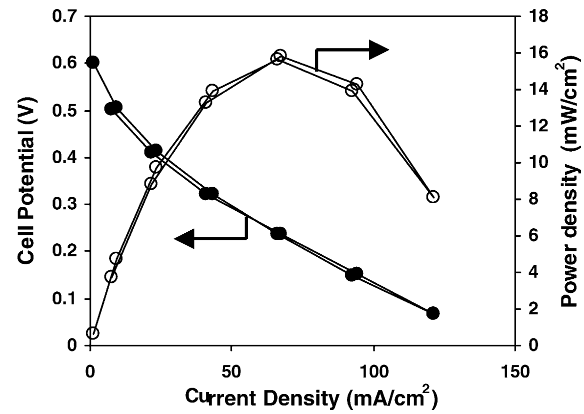

Fig. 8. *IV* (dark circle) and power density (clear circle) profiles of a Si-μFC operating with 0.5 ml/min of 10 M HCOOH and 90 ml/min of humidified oxygen at room temperature and atmospheric pressure. The distance between the Au electrode and the Nafion membrane is 2 μm.

To overcome these issues, the cell is often operated at higher temperature, and Pt/Ru is used as the catalyst to avoid the CO poisoning issue [17,26]. An OCP of roughly one-third of EMF is indicative of mixed potentials at the electrodes, most likely due to fuel crossover to the cathode side [4,20,21]. Employing a thicker Nafion membrane could reduce crossover in both liquid fuel systems, although that would also increase the internal resistance in the cell.

3.4. Performance: HCOOH–oxygen testing

Waszczuk et al. [23] and Lu et al. [24] have investigated the electro-oxidation of HCOOH on Pt and Pt–Pd. Two possible pathways for the oxidation of formic acid on platinum have been proposed: dehydrogenation and dehydration. The dehydrogenation pathway in which HCOOH is directly oxidized to CO_2 is believed to dominate over the kinetically slower dehydration pathway, which goes through the formation of the unwanted catalyst poisoning CO intermediate. The overall oxidation reaction at the anode is

$$HCOOH \rightarrow CO_2 + 2H^+ + 2e^- \qquad (2)$$

In the present work, the concentration of formic acid is chosen as 10 M with a flow rate of 1 ml/min, while the humidified oxygen is fed to cathode under the same condition as the methanol case. Formic acid concentrations higher than 10 M reduced the OCP due to increase in cell resistance [20]. With the HCOOH at 10 M, the OCP is approximately 0.55 V and peak powers as high as 17 mW/cm^2 at 0.25 V were reached at room temperature (see Fig. 8). The maximum current density of the Si-μMEA when running on 10 M formic acid is approximately 135 mA/cm^2. These current and power densities at room temperature are very similar to the exact same cell operating with 1.25 M MeOH at 60 °C demonstrating the attractiveness of formic acid as a fuel source. Note that the highly concentrated formic acid (10 M) can be used due to reduced crossover at room temperature in comparison to the methanol case [20].

The OCP (∼0.55 V) in these formic acid FC tests is significantly lower than the theoretical EMF of 1.45 V. Similar to the methanol fuel cell case, this reduced OCP is typically attributed to fuel crossover through the membrane to the cathode by means of diffusion and electro-osmotic drag and to catalyst poisoning. In the Si-μMEAs fabricated in this study, thin Nafion 112^{TM} membranes (thickness of ∼50 μm) have been employed, easing the crossover of fuel to cathode. According to literature, it is unclear, however, whether fuel crossover is caused by the direct diffusion of HCOOH or through the occurrence of side reactions replacing HCOOH with MeOH, which is known to crossover more readily than formic acid [20]. In addition, experimental observations indicate that poisoning of the catalyst also contributes to the low OCP in the Si-μMEA. Though the direct oxidation of HCOOH into CO_2 is favored in the anode reaction, decomposition of formic acid into CO, a known poisoning agent, can still occur through the second reaction pathway for HCOOH on pure Pt catalyst [16,20]. Further improvements to our catalyst formulation, e.g. using Pt/Pd catalyst [23,24], can increase the HCOOH oxidation activity and is expected to greatly improve the cell performance by increasing both its OCP and cell current density.

Several other performance-related issues that have previously been addressed in traditional PEMFC system but have not yet been addressed in the design and operation of the Si-μMEA fuel cells studied here include: (i) the exclusion of O_2 from the anode to supply oxygen-free fuel and to reduce mixed potential at the anode; (ii) the exhaust rate of CO_2 from the anode, both of which can reduce the power output; (iii) the decrease in power output due to increased resistance as a result of edge collection of current and uneven contact of the catalyst-current collector on the PEM; (iv) reduced or uneven fuel transport to the anode; and (v) the rejection of excess water from the cathode. Each of these issues can act, to some, yet unknown extent, in reducing the power density over that of traditional PEMFC designs.

4. Conclusion

We have demonstrated a silicon-based microfabricated MEA design that is expected to have certain advantages over the traditional approach to fabrication and assembly. Mesh-type electrode design allows faster transport of fuels and byproducts in comparison to the traditional MEAs relying on the pore-diffusion in the gas diffusion layer. Electrodepositing Pt catalyst directly on the gold current collector reduces electron resistance in the cell. The performance characterization of the Si-μMEA was carried out by testing with three different fuels: H_2, MeOH, and HCOOH. As expected, the hydrogen gas fuel cell achieved the highest power densities of the three fuel combinations due to higher transport rates, fast reaction kinetics, low crossover, and the absence of catalyst poisoning. Microscale silicon-based PEMFCs running on HCOOH at room temperature appear to offer a number of advantages due to an order of magnitude faster kinetics than MeOH, and many orders of magnitude higher energy density than H_2. The use of unoptimized catalysts, a thin Nafion 112^{TM} membrane, and various other factors limit the performance in the two liquid fuel cases. In ongoing work, which we will report shortly, we have been able to address some of these limitations.

Acknowledgements

This work was supported by the Defense Advanced Projects Research Agency under US Air Force Grant F33615-01-C2172. All SEM work was conducted in the Center for Microanalysis of Materials, in the Frederick Seitz Material research Laboratory, University of Illinois, which is partially supported by the U.S. Department of Energy under grant DEFC02-91-ER45439. Any opinions, findings, and conclusions or recommendations expressed in this publication are those of the authors and do not necessarily reflect the views of the Department of Energy, the US Air Force, or the Defense Advanced Projects Research Agency.

References

[1] S.C. Kelley, G.A. Deluga, W.H. Smyrl, A miniature methanol/air polymer electrolyte fuel cell, Electrochem. Solid-State Lett. 3 (2000) 407–409.
[2] S.C. Kelley, G.A. Deluga, W.H. Smyrl, Miniature fuel cells fabricated on silicon substrates, AIChE J. 48 (2002) 1071–1082.
[3] A. Heinzel, C. Herbling, M. Muller, M. Zedda, C. Muller, Fuel cells for low power applications, J. Power Sources 105 (2002) 250–255.
[4] W.Y. Sim, G.Y. Kim, S.S. Yang, Fabrication of micro power source (MPS) using a micro direct methanol fuel cell (μDMFC) for the medical application, in: IEEE International Conference On MEMS, Technical Digest, 14, 2001, pp. 341–344.
[5] M.N. Mench, Z.H. Wang, K. Bhatia, C.Y. Yang, Design of a micro direct methanol fuel cell, in: Proceeding of ASME International Mechanical Engineering Congress Exposotion, 2001, pp. 317–324.
[6] H.L. Maynard, J.P. Meyers, Miniature fuel cells for portable power: design considerations and challenges, J. Vac. Sci. Technol. B 20 (2002) 1287–1297.
[7] A. Jansen, S. van Leeuwen, A. Stevels, Design of a fuel cell powered radio, a feasibility study into alternative power sources for portable products, in: IEEE International Symposium on Electronics and the Environment, 2000, pp. 155–160.
[8] E.R. Choban, L.J. Markoski, P.J.A. Kenis, Microfluidic fuel cells based on laminar flow, J. Power Sources 128 (1) (2004) 54–60.
[9] K. Shah, W.C. Shin, R.S. Besser, Novel microfabrication approaches for directly patterning PEM fuel cell membranes, J. Power Sources 123 (2003) 172–181.
[10] K. Shah, W.C. Shin, R.S. Besser, A PDMS micro proton exchange membrane fuel cell by conventional and non-conventional microfabrication techniques, Sens. Actuatators B 97 (2004) 157–167.
[11] J.D. Morse, A.F. Jankowski, R.T. Graff, J.P. Hayes, Novel proton exchange membrane thin-film fuel cell for microscale energy conversion, J. Vac. Sci. Technol. A 18 (4) (2000) 2003–2005.
[12] J. Yu, P. Cheng, Z. Ma, B. Yi, Fabrication of a miniature twin-fuel-cell on silicon wafer, Electrochim. Acta 48 (2003) 1537–1541.
[13] J. Yu, P. Cheng, Z. Ma, B. Yi, Fabrication of miniature silicon fuel cells with improved performance, J. Power Sources 124 (2003) 40–46.
[14] S.J. Lee, A. Chang-Chien, S.W. Cha, R. O'Hayre, Y.I. Park, Y. Saito, F.B. Prinz, Design and fabrication of a micro fuel cell array with flip-flop interconnection, J. Power Sources 112 (2002) 410–418.
[15] K.B. Min, S. Tanaka, M. Esashi, Silicon-based micro-polymer electrolyte fuel cells, IEEE International Conference On MEMS, Technical Digest, 16 (2003) 379–382.
[16] Y.H. Seo, Y.H. Cho, A miniature direct methanol fuel cell using platinum sputtered microcolumn electrodes with limited amount of fuel, IEEE International Conference On MEMS, Technical Digest, 16 (2003) 375–378.
[17] T.J. Yen, N. Fang, X. Zhang, G.Q. Lu, C.Y. Yang, A micro methanol fuel cell operating at near room temperature, Appl. Phys. Lett. 83 (19) (2003) 4056–4058.
[18] D. Aurbach, Y. Gofer, Z. Lu, A. Schechter, O. Chusid, H. Gizbar, Y. Cohen, V. Ashkenazi, M. Moshkovich, R. Turgeman, E. Levi, A short review on the comparison between Li battery systems and rechargeable magnesium battery technology, J. Power Sources 97/98 (2001) 28–32.
[19] L. Carrette, K.A. Friedrich, U. Stimming, Fuel cells: principles, types, fuels, and applications, Chem. Phys. Chem. 1 (2000) 162–193.
[20] C.A. Rice, S. Ha, R.I. Masel, P. Waszczuk, A. Wieckowski, T. Barnard, Direct formic acid fuel cells, J. Power Sources 111 (2002) 83–89.
[21] S. Ha, C.A. Rice, R.I. Masel, A. Wieckowski, Methanol conditioning for improved performance of formic acid fuel cells, J. Power Sources 112 (2002) 655–659.
[22] Y. Zhu, S.Y. Ha, R.I. Masel, High power density direct formic acid fuel cells, J. Power Sources 130 (2004) 8–14.
[23] P. Waszczuk, T.M. Barnard, C. Rice, R.I. Masel, A. Wieckowski, A nanoparticle catalyst with superior activity for electro-oxidation of formic acid, Electrochem. Commun. 4 (2002) 599–603.
[24] G. Lu, A. Crown, A. Wieckowski, Formic acid decomposition on polycrystalline platinum and pallidized platinum electrodes, J. Phys. Chem. 103 (1999) 9700–9711.
[25] Y. Rhee, S. Ha, R.I. Masel, Crossover of formic acid through nafion membranes, J. Power Sources 117 (2003) 35–38.
[26] D. Kim, E.A. Cho, S.A. Hong, I.H. Oh, H.Y. Ha, Recent progress in passive direct methanol fuel cells at KIST, J. Power Sources 130 (2004) 172–177.
[27] A. Hamnett, in: Andrzej Wieckowski (Ed.), Mechanism of Methanol Electro-oxidation, Interfacial Electrochemistry: Theory, Experiment, and Applications, Marcel Dekker, New York, 1999, pp. 843–883.

Biographies

J. Yeom is a PhD student in the Department of Mechanical & Industrial Engineering at the University of Illinois. His research interests are in the fabrication and characterization of novel microfluidic systems.

G.Z. Mozsgai joined Renew Power Inc. after graduation with a MS in the Mechanical Engineering from the University of Illinois. He is currently developing a miniaturized formic acid fuel cell system.

B.R. Flachsbart, PhD in Electrical Engineering from UIUC, is presently a research scientist in the Department of Mechanical & Industrial Engineering at the University of Illinois. His research interests include the fabrication and characterization of optoelectronic and microfluidic systems with applications in the area of BioMEMS.

E.R. Choban received his PhD in Chemical & Biomolecular Engineering from the University of Illinois. His research included the development of laminar flow-based membraneless microfuel cell as well as the characterization of silicon-based miniature fuel cell systems. He joined 3M in January of 2005.

A. Asthana obtained his PhD in Chemistry from Bhopal University, India, and was a postdoc at UIUC working on silicon-based microfuel cells. Presently he is a research scientist at Chungnam National University, Korea. His research interests include the application of microfluidics for biofuel cells, microanalysis systems, and microreactors.

M.A. Shannon received a PhD in mechanical engineering from UC Berkeley. He is currently a professor of Mechanical & Industrial Engineering at the University of Illinois since 1994 and an affiliate of the Beckman Institute for Advanced Science and Technology with appointments in electrical and computer Engineering as well as bioengineering. His current field of research is MEMS and microfabrication technologies, including the fabrication of biosensors.

P.J.A. Kenis received a PhD in Chemical Engineering from Twente University, The Netherlands and is currently an assistant professor of Chemical & Biomolecular Engineering at the University of Illinois since 2000 with affiliate appointments in the Beckman Institute, the Institute for Genomic Biology, and the department of Mechanical & Industrial Engineering. His research utilizes microfabrication and micro/nanofluidics in the development of microchemical systems: microreactors for fuel reforming or biocatalysis, microfuel cells, and a wide range of microfluidic tools for biological studies.